23rd ABCM International Congress of Mechanical Engineering
December 6-11, 2015, Rio de Janeiro, RJ, Brazil

PRESSURE COEFFICIENT DISTRIBUTION AT THE TEST SECTION OF THE TA-2 WIND TUNNEL

Daniel Simão Alves de Lima
Maria Luisa Colucci da Costa Reis
Marcos da Silva e Souza
Praça Marechal do Ar Eduardo Gomes,número 50 Vila das Acácias, São José dos Campos - SP, Brazil
danieldsal@iae.cta.br
marialuisamccr@iae.cta.br
marcossouzamss@iae.cta.br
Abstract. *This paper presents the results of the pressure distribution on the upper and lateral walls of the test section in the Wind Tunnel number 2, TA-2, of the Aerodynamics Division of the Institute of Aeronautics and Space, IAE/ALA. It is the first step of the campaign carried out to analyze the flow properties in the TA-2. The measured parameters are static and dynamic pressures of the airflow, which are the input quantities of the mathematical model used for estimation of the pressure coefficient, which is the output quantity. The measurement of static pressures at the test section walls is accomplished by positioning slats along the superior and lateral walls. Pressure taps located on the slats are connected to pressure scanners to supply local relative static pressure measurements. Pitot tubes located on the upper wall at the beginning of the test section supply dynamic and total pressure measurements. Data reduction includes the evaluation of the uncertainties associated with the measured quantities as well as their propagation to the output quantity. Least squares fitting is applied to the experimental data in order to supply pressure coefficient distribution as a function of longitudinal positions of the test section. The quality of the fit is evaluated by the chi-squared quantity. International standardization recommended by metrological organizations is followed for uncertainty evaluation. The TA-2 calibration curves supplied by this study can be used in the development of methods for airflow corrections, such as wall interference corrections by pressure signature. Results revealed a pressure gradient downstream of the TA-2 test section.*

Keywords: *Pressure coefficient, flow quality, wind tunnel, least squares fitting*

1. INTRODUCTION

Wind tunnels are experimental facilities designed to simulate flows around structures under aerodynamic loads. The metrological reliability of the data originating from wind tunnel tests depends on the knowledge of the quality of the flow properties in the test section. Aiming the calibration of the airflow in the test section of the subsonic wind tunnel TA-2 (Fig. 1), a test campaign is being carried out. This includes the analysis of the pressure distribution at the test section, considering near wall regions, the boundary layer growth and turbulence level.

Figure 1. Aerial view of the aerodynamics division. The TA-2 wind tunnel circuitry is seen on the left.

This paper presents test results of the pressure coefficient distribution C_p on the walls of the test section of the wind tunnel TA-2. Data acquisition supplied differential static pressures Δp in 9 aluminum slats fixed on the walls and freestream dynamic pressures q_∞. The velocity regimes covered by the tests are related to 50, 100, 200, 300, 400, 500 and 600 mmH_2O. In this paper the results refer to 300 mmH_2O, typical for variety of tests conducted at the TA-2 wind tunnel. The presented procedure can be extended to the remaining velocities.

Information on the pressure coefficient distribution provides a mean to control and optimize the quality of the flow and can be used in the development of a methodology for wall interference correction (Barlow *et al.*, 1999).

2. METHODOLOGY

In this section we describe the test configuration, the instrumentation, the mathematical model and the curve fitting method. A rationale of the pressure distribution expected in the wind tunnel test section is also shown.

2.1 Static Pressure Taps

The static pressures in the test section are evaluated employing aluminum slats fixed on the walls with 36 pressure taps aligned along the x axis (Fig. 2). The nine aluminum slats are named in ascending order from right to left walls passing by the ceiling as show in Fig. 3, where: L1 $\rightarrow$ below right, L2 $\rightarrow$ central right, L3 $\rightarrow$ upper right, L4 $\rightarrow$ right ceiling, L5 $\rightarrow$ central ceiling, L6 $\rightarrow$ left ceiling, L7 $\rightarrow$ upper left, L8 $\rightarrow$ central left and L9 $\rightarrow$ below left.

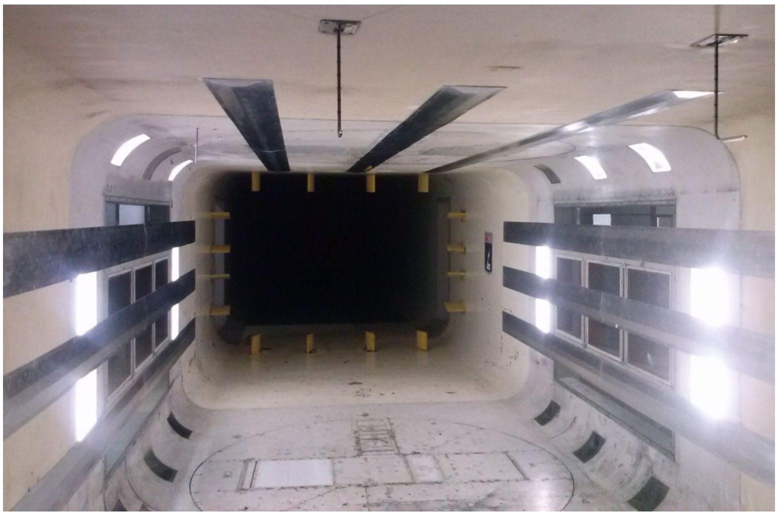

Figure 2. TA-2 test section instrumented with pressure taps in aluminum slats. Upstream of the flow we can see two Pitot tubes on the ceiling.

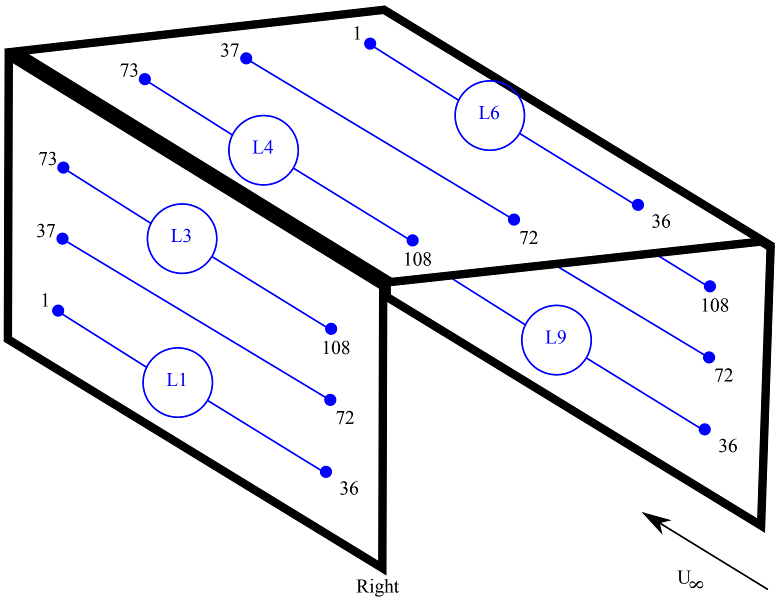

Figure 3. Naming and numbering for aluminum slats and pressure taps. U_∞ indicates wind direction.

Each aluminum slat is composed of two parts with 18 pressure taps. The pressure tap positioning for L1 is shown in Fig. 4, where the center of the wind tunnel test section is the origin of the x axis.

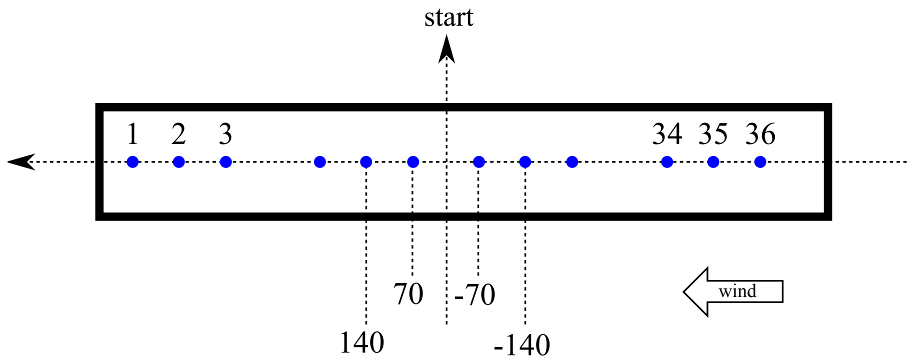

Figure 4. The x-coordinates and numbering of the L1 aluminum slat pressure taps.

2.2 Instrumentation

The static pressures on the slats pressure taps are measured by three Scanivalve pressure scanners (Fig. 5). Each scanner has 64 channels. The taps are connected to instrumentation through plastic tubing (Fig. 6).

Figure 5. Static pressure scanner.

The three pressure scanners are calibrated using the DPI 610 Pressure Calibrator (Fig. 7).

The dynamic pressures are supplied by Pitot tubes positioned on the upper wall of the test section as show in Fig. 2.

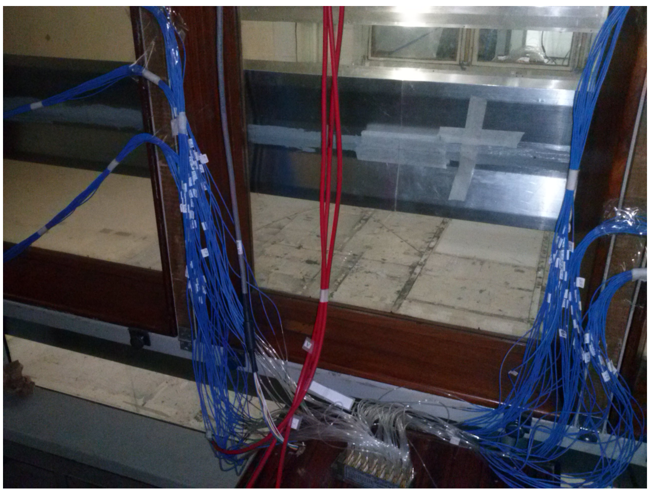

Figure 6. Tubing connecting the pressure taps to instrumentation.

Figure 7. Standard instrument used to calibrate the pressure scanners.

A calibration code was elaborated in LabView® to reduce calibration data. Display of the 192 signals originated from the pressure channels is given as output.

During calibration, pressure is applied to the pressure scanners at approximately 0, 15, 30, 50, 65 and 80% of the full scale of the instrument. The readings are carried out for negative and positive pressures, totalizing 11 calibration points. The acquisition system is configured for a 11 kHz frequency rate. The acquisition for a single data point lasts 20 s. For each one of the 11 data points, a single channel of the pressure scanner is swept 30 times. Each swept is composed of 100 readings. Data is stored in text format and exported to MatLab® for data reduction. Least squares fitting is applied to calibration data to supply linear and angular coefficients of first degree polynomials.

2.3 Mathematical Model

To estimate the pressure coefficient distribution, C_p, in each pressure tap for the ceiling and the left and right walls, the mathematical expression used is Eq. (1):

$$C_p = \frac{p - p_\infty}{q_\infty} = \frac{\Delta p}{q_\infty} \tag{1}$$

where,

$\Delta p = p - p_\infty$ is the difference between the local static pressure, p, and the freestream static pressure, p_∞;

q_∞ is the freestream dynamic pressure measured by differential pressure sensor connected to a Pitot tube.

Negative values of C_p represent static pressures, p, lower than the freestream static pressure, p_∞.

The evaluation of the uncertainty associated to the pressure coefficient, u_{C_p}, is obtained by employing the Law of propagation of uncertainty, expressed by (BIPM *et al.*, 2008):

$$u_y^2 = \sum_{i=1}^{N} \left(\frac{\partial y}{\partial x_i} \right)^2 u^2(x_i) \tag{2}$$

were y is the output quantity, named measurand (BIPM *et al.*, 2012), and x_i are the input quantities of the experiment.

Applying Eq. (2) to Eq. (1) results in:

$$u_{C_P}^2 = \left(\frac{\partial C_P}{\partial \Delta_P} \right)^2 u_{\Delta_P}^2 + \left(\frac{\partial C_P}{\partial q_\infty} \right)^2 u_{q_\infty}^2 \tag{3}$$

$$u_{C_P}^2 = \left(\frac{1}{q_\infty} \right)^2 u_{\Delta_P}^2 + \left(\frac{-\Delta_P}{q_\infty^2} \right)^2 u_{q_\infty}^2 \tag{4}$$

where $u_{\Delta p}$ and u_{q_∞} are quantified by the standard deviations of the pressure signals, expressed by:

$$S = \sqrt{\frac{\sum_{i=1}^{N} (x_i - \overline{x})^2}{N - 1}} \tag{5}$$

2.4 Curve fitting to data points

The curve fitting to experimental data is carried out by using the least squares method. This process supply the calibration curves of the pressure distribution on the wind tunnel walls. The mathematical model of the fit must be investigated. If a uniform distribution is expected in the test section, a first degree polynomial must be fitted to the C_p estimated values:

$$y = a_0 + a_1 x \tag{6}$$

were y is related to C_p, a_0 and a_1 are the polynomial parameters and x is the longitudinal distance in the test section, measured in millimeters according to Fig. 4. Applying the Law of propagation of uncertainty in Eq. (6) one obtains the inferior and superior uncertainty limit curves, expressed by:

$$\begin{aligned} u_y^2 = & \left(\frac{\partial y}{\partial a_0}\right)^2 u_{a_0}^2 + \left(\frac{\partial y}{\partial a_1}\right) u_{a_1}^2 + \left(\frac{\partial y}{\partial x}\right)^2 u_x^2 \\ & + 2\left[\left(\frac{\partial y}{\partial a_0}\right)\left(\frac{\partial y}{\partial a_1}\right) u(a_0, a_1) + \left(\frac{\partial y}{\partial a_0}\right)\left(\frac{\partial y}{\partial x}\right) u(a_0, x) + \left(\frac{\partial y}{\partial a_1}\right)\left(\frac{\partial y}{\partial x}\right) u(a_1, x)\right] \end{aligned} \tag{7}$$

Considering the uncertainty in the quantity x, u_x, the covariance between a_0 and x, $u(a_0, x)$, and the covariance between a_1 and x, $u(a_1, x)$, null, Eq. (7) results in:

$$u_y^2 = (1)^2 u_{a_0}^2 + (x)^2 u_{a_1}^2 + 2(1)(x)u(a, b) \tag{8}$$

The quality the fitting is quantified by the chi-squared, χ^2:

$$\chi^2 = \sum_{j=1}^{n} \left(\frac{y_j - y_{j_{fit}}}{u_{y_j}}\right)^2 \tag{9}$$

The value of the $y_{j_{fit}}$ is the value of the estimated C_P obtained from the curve fitting. Each aluminum slat will have its own χ^2 value.

The estimated value obtained in Eq. (9) depends on the uncertainties u_{y_j} associated to the measured quantities y_j. Incorrect assignment of the uncertainties u_{y_j} will lead to incorrect values of χ^2 (Bevington and Robinson, 2003). The magnitude of χ^2 is also determined by the selected function y_{fit}.

If we divide the χ^2 value by the number of degrees of freedom of the fitting, ν, we will have the reduced chi-squared as $\chi_\nu^2 \equiv \chi^2/\nu$. A reduced chi-squared around 1 indicates good quality of fitting, either in terms of the chosen function or in terms of the assigned uncertainties in data points.

2.5 The expected pressure coefficient distribution

The test section of a wind tunnel is designed to present uniform airflow velocity, V. If the velocity distribution is uniform, the dynamic pressure, q, is constant:

$$q = \frac{1}{2}\rho V^2 \tag{10}$$

where ρ is the airflow density.

According to Bernoulli's equation, (Barlow *et al.*, 1999), the total pressure, $p_0 = p + q$, is constant in two locations of the airflow:

$$p_2 + \rho\frac{V_2^2}{2} = p_1 + \rho\frac{V_1^2}{2} \tag{11}$$

$i.e.$, the sum of static, p, and dynamic, q, pressures is constant.

Interaction between the airflow and the solid wall of the wind tunnel causes a boundary layer growth downstream the test section, causing a decrease in the effective free stream cross sectional area outside the boundary layer. Considering two cross sectional areas upstream and downstream of the test section, A_1 and A_2 respectively, and applying the continuity equation for incompressible,constant density flow:

$$\rho_1 V_1 A_1 = \rho_2 V_2 A_2 \tag{12}$$

the effective A_2 area is decreased due to the boundary layer, leading to an increase in V_2 velocity. In order to maintain uniform velocity, the wind tunnels are designed with divergent walls, that is, the cross area at the beginning of the test section, A_1, is smaller than the cross area at the end of the test section, A_2.

3. Results and discussion

The results presented in this paper are for velocities related to 300 mmH_2O. The pressure coefficient distribution at the 36 pressure taps obtained on the slats of the right wall, L1, L2, and L3, are presented in Fig (8). The nominal test section is limited by the distances -1610 and 1610 mm. It encompasses 24 pressure taps but only 23 were considered in the curve fitting. The point -1610 mm was discarded due to disturbances caused by the ramp shape at the beginning of the slats. Wind direction is from right to left.

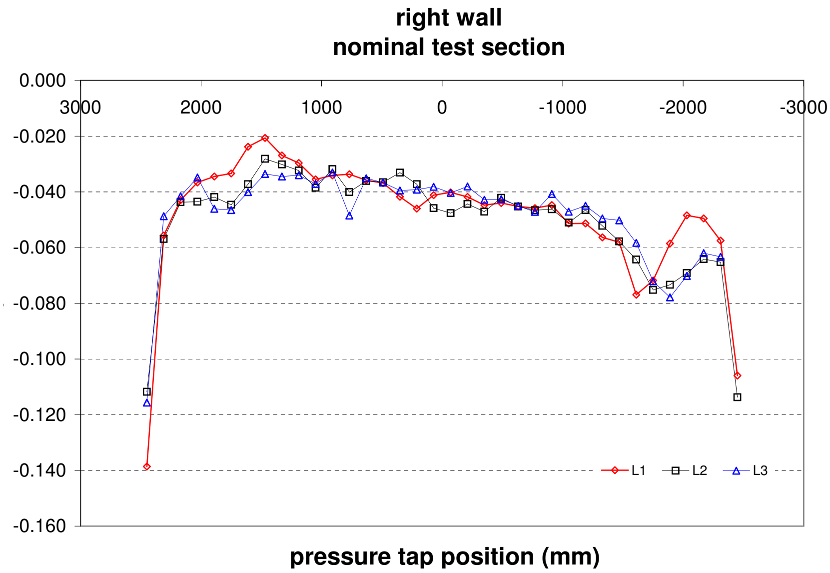

Figure 8. Pressure coefficient distribution, C_p, on the right wall.

3.1 The C_p distribution and associated uncertainties

The pressure coefficient, C_p, and the associated uncertainty, u_{C_p}, on the right wall of the nominal test section are presented in Fig. (9). The u_{C_p} values are estimated by using Eq. (4).

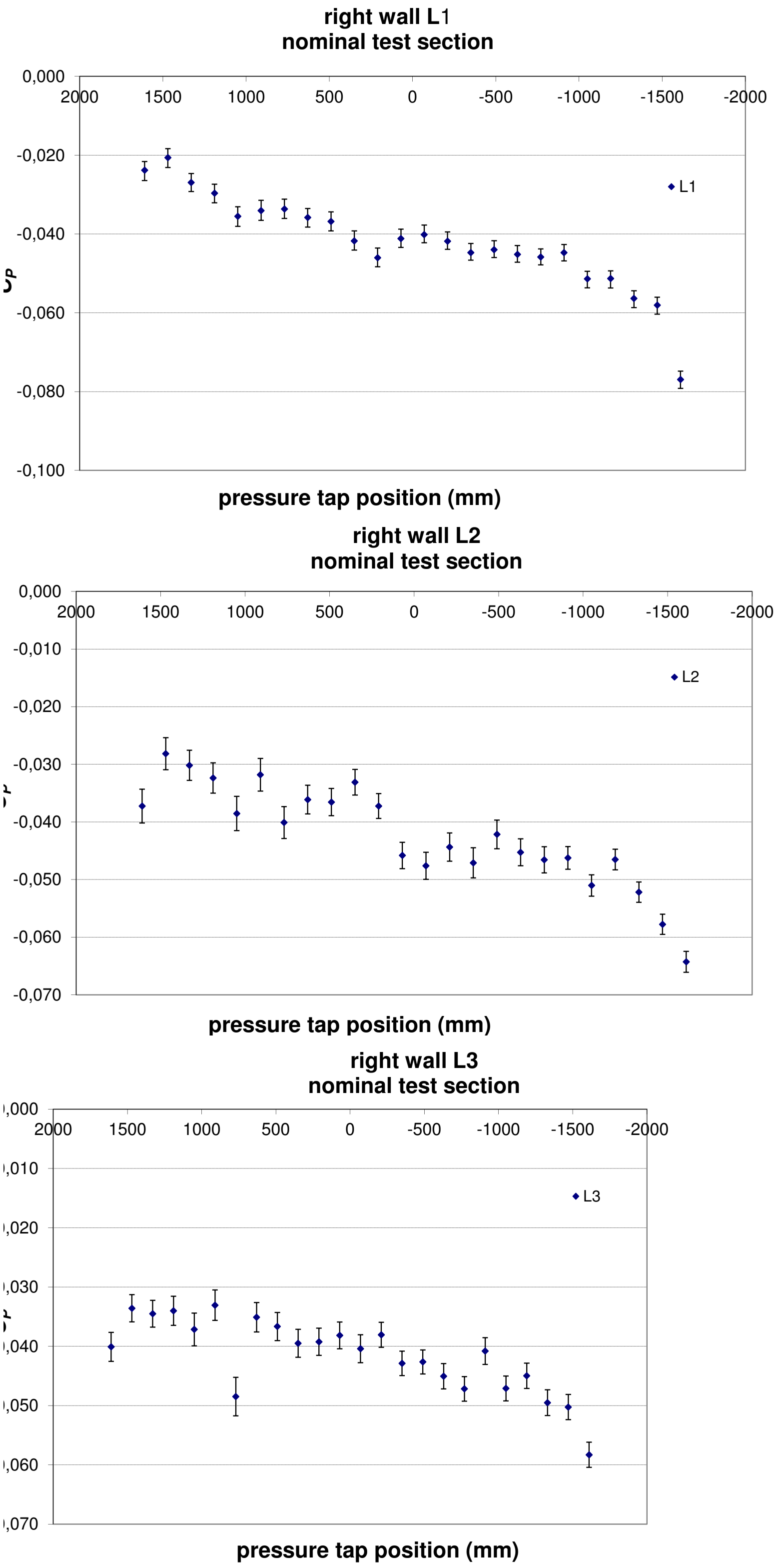

Figure 9. Pressure coefficient distribution, C_p, and associated uncertainty u_{C_p} on the right wall.

3.2 Calibration curves

First degree polynomials $C_p = a_0 + a_1 x$, were fitted to the pressure coefficient values obtained in each pressure tap. The curve fitting was done by employing the least squares method in matricial formalism which supplies the variances and covariances of the fitted parameters a_0 and a_1. The calibration curves are presented in Tab. 1. Ideally, the wind tunnel test section should present a gradient-free calibration curve, $i.e.$, the angular coefficient a_1 should be equal to zero. According to Tab. 1, one concludes that the static pressure p_2 increases and the Δp value becomes less negative, that is, C_p is less negative at the end of the test section. Increase of pressure downstream the flow near the wall is due to the divergency on the lateral walls of the TA-2 test section, estimated to compensate boundary layer effects. Intensity of the pressure increase near the divergent walls must be correlated to the size of the boundary layer in order keep the ideal conditions of constant pressure and velocity through the test section in area equivalence to that of the beginning of the test section.

Further studies during this campaign will correlate the size of the boundary layer with the necessary pressure increase at the walls.

Table 1. Calibration curves of the pressure coefficient C_p on the right wall.

Slat	Equation
L1	$C_p = -409(4) \times 10^{-4} + 95(5) \times 10^{-7} x$
L2	$C_p = -426(7) \times 10^{-4} + 76(5) \times 10^{-7} x$
L3	$C_p = -409(4) \times 10^{-4} + 46(5) \times 10^{-7} x$

3.3 Uncertainty in the calibration curves

Using (8), one estimates the uncertainty in the fitted curves, $u_{C_{p_{fit}}}$. The least squares fit was done considering the uncertainty in data points as shown in Fig. 9 and using Eq. (4). This procedure results in Fig. 10 for the right wall. The superior and inferior uncertainty curves correspond to a 95% level of confidence, $i.e.$, the $u_{C_{p_{fit}}}$ values were multiplied by 2.

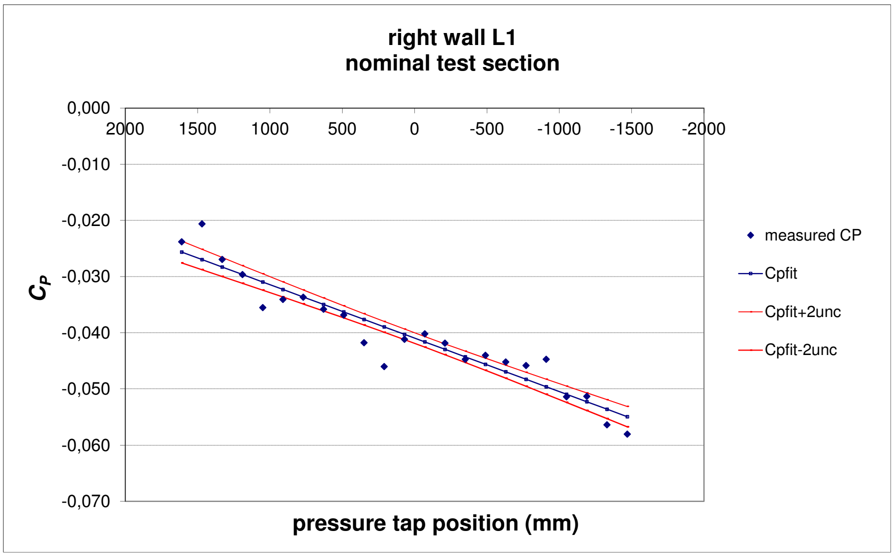

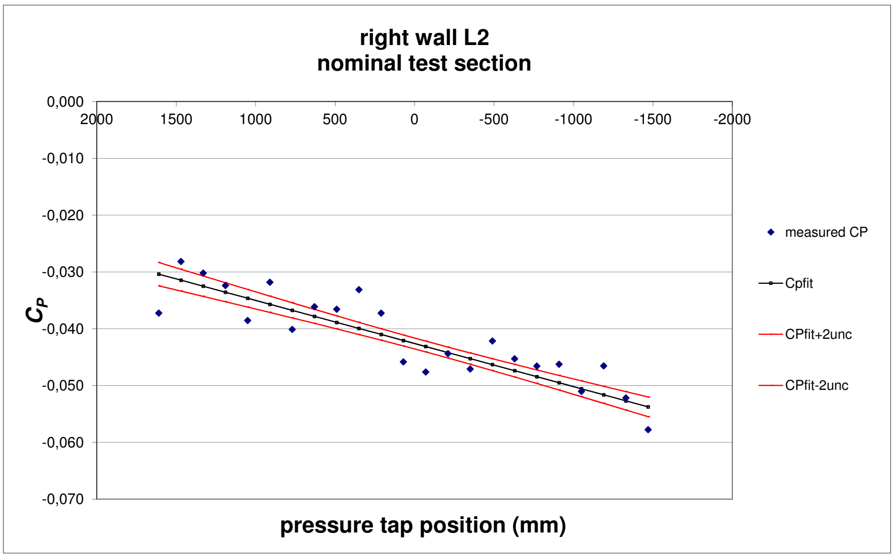

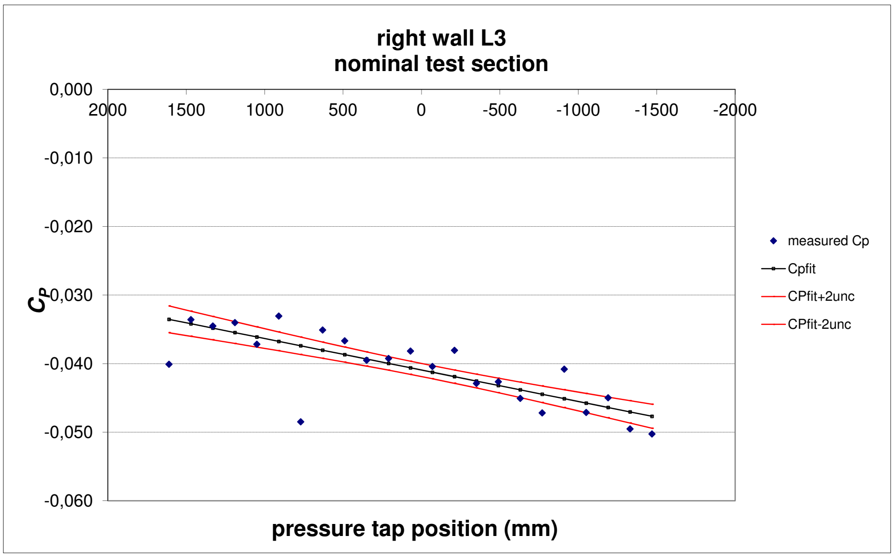

Figure 10. Calibration curves of the right wall for the nominal test section. Uncertainty limits with a 95 % of level of confidence.

3.4 Quality of the curve fitting

The quality of the fitting was evaluated in relation to the chosen curve and the associated uncertainties of the experimental data. The employed method to fit the curve to the experimental data was the least squares fitting. We chose a first degree polynomial to fit the pressure coefficient distribution, C_p, along the walls of the TA-2 test section. For the uncertainties associated to the pressure coefficients, $u_{C_{p_{measured}}}$, we used the standard deviation of the measurements supplied by the pressure taps. Table 2 shows the chi-squared, χ^2, and reduced chi-squared, χ^2_ν, for the fitting in the right wall slats. The obtained values indicate that the numerator and the denominator in Eq. (9) are equilibrated, resulting in χ^2_ν next to one.

Table 2. Quality of the fitting.

Right wall			
	L1	L2	L3
χ^2	36.63	54.16	100.03
χ^2_ν	1.74	2.58	4.76

4. CONCLUSIONS

The pressure coefficient distribution on the walls of the TA-2 test section was evaluated. Results revealed a pressure gradient downstream of the test section. Calibration curves were supplied considering uncertainty in experimental data. Uncertainty limits of the calibration curves were also supplied. The results can be used to improve the airflow quality of the wind tunnel and in the development of wall corrections.

5. REFERENCES

Barlow, J., Rae, W. and Pope, A., 1999. *Low-Speed Wind Tunnel Testing*. Aerospace engineering, mechanical engineering. Wiley. ISBN 9780471557746.

Bevington, P. and Robinson, D., 2003. *Data reduction and error analysis for the physical sciences*. McGraw-Hill Higher Education. McGraw-Hill. ISBN 9780072472271.

BIPM, I., IFCC, I., IUPAC, I. and ISO, O., 2012. "The international vocabulary of metrology—basic and general concepts and associated terms (vim), 3rd edn. jcgm 200: 2012". *JCGM (Joint Committee for Guides in Metrology)*.

BIPM, I., IFCC, I. and IUPAC, I., 2008. "Oiml. evaluation of measurement data guide to the expression of uncertainty in measurement jcgm 100: 2008 (gum 1995 with minor corrections)".

6. RESPONSIBILITY NOTICE

The authors are the only responsible for the printed material included in this paper.